ELSEVIER

Journal of Chromatography A, 960 (2002) 209–220

JOURNAL OF CHROMATOGRAPHY A

www.elsevier.com/locate/chroma

# Study of flow profile distortions and efficiency in counter pressure moderated partial filling micellar electrokinetic chromatography in relation to the relative buffer zone lengths

Daniela Michalke, Thomas Welsch*

*University of Ulm, Department of Analytical and Environmental Chemistry, Albert-Einstein-Allee 11, D-89081 Ulm, Germany*

**Abstract**

The influence of the relative buffer zone lengths on the efficiency was investigated in partial filling micellar electrokinetic chromatography using sodium dodecyl sulfate as separation additive. Varying relative zone lengths were obtained by applying identical initial separation zone lengths but different total lengths of the capillaries. Plate numbers of a homologous series of ω-phenylalcohols were measured to indicate the effect of both a changing relative zone length during the run and a counter pressure applied on the cathodic buffer reservoir. The magnitude and the course of these plate numbers are discussed on the basis of models for flow profile superposition and flow profile deformation which are caused by an intersegmental pressure arising at the boundary between the two buffer zones with different electroosmotic flow velocities. Calculation of the intersegmental pressure and of the resulting laminar flow components in the buffer zones on the basis of some equations for electroosmotic and hydrodynamic flow supported the interpretation that a long background buffer zone should be avoided in case of mismatched electroosmotic flows. 

*Keywords:* Partial filling micellar electrokinetic chromatography; Relative buffer zone length; Flow profile superposition; Counter pressure; Micellar electrokinetic chromatography; Efficiency

## 1. Introduction

Due to its superior efficiency micellar electrokinetic chromatography (MEKC) or more generally electrokinetic chromatography (EKC) has proven to be an interesting alternative to high-performance liquid chromatography for the separation of charged and neutral analytes. During the past years the spectrum of the applied separation additives has been expanded from the initially used sodium dodecyl sulfate (SDS) [1] to other types such as cyclodextrins, dendrimers, polymeric additives, and charge-transfer interacting additives in order to achieve special selectivities [2–14].

But the wide applicability of EKC is still reduced by a limited migration time window and by an interference of some separation additives with detection [14–22]. Both problems can be overcome by the application of a partial filling (PF) technique in connection with counter pressure [12–14,16,19,20]. This method includes the filling of the capillary with two buffer plugs: a separation buffer (SB) containing the separation additive and a background buffer (BB) which does not interfere detection. The common movement of the separation buffer zone towards the detection window during the run can be slowed down or counterbalanced by an appropriate counter

*Corresponding author. Tel.: +49-731-5022-751; fax: +49-731-5022-752.

*E-mail address:* thomas.welsch@chemie.uni-ulm.de (T. Welsch).

0021-9673/02/$ – see front matter 
PII: S0021-9673(01)01394-2

pressure, $p_{cp}$. A negative concomitant of the partial filling technique is a flow-equalizing intersegmental pressure, $p_i$, arising at the boundary between the two buffer zones in case their electroosmotic flow velocities are different. This pressure induces a parabolic flow profile distortion in each buffer zone which gives rise to additional band broadening. The dramatic influence of such flow profile distortions on efficiency in case of mismatched buffer concentrations and the influence of counter pressure was reported in a previous paper [16]. Maximum plate numbers were obtained only in case of adapted electroosmotic flow velocities of the two buffer zones.

Dispersion attributed to axially non-uniform electroosmotic flows has also been reported by other research groups in case of different buffer compositions and/or concentrations in capillary zone electrophoresis (CZE) [23], MEKC [24] and PF-(M)EKC [25,26], in case of axially non-uniform $\zeta$-potentials of different origin in CZE [27–30] and in case of capillary electrochromatography (CEC) [31].

In this work we studied both the influence of an initial difference in the relative buffer zone lengths and the influence of the change of the relative buffer zone lengths during the run on efficiency for the case of non-adapted electroosmotic flow velocities ($u_{eo,SB} < u_{eo,BB}$) and for the case of identical electroosmotic flow velocities of the two buffer zones. Different initial filling degrees (40 and 60%) were realized by a constant length of the separation buffer zone in combination with different total lengths of the capillaries.

## 2. Theoretical considerations

In practical partial filling EKC the separation buffer is most often prepared by just adding the separation additive to the background buffer. Therefore, owing to its higher ionic strength, the electroosmotic flow velocity of the separation buffer, $u_{eo,SB}$, will be lower than the electroosmotic flow velocity of the background buffer, $u_{eo,BB}$. When using such a buffer combination the difference between the electroosmotic flow velocities will produce a flow-equalizing intersegmental pressure, $p_i$, which in this case must be lower than the ambient pressure, $p_{atm}$, in order to accelerate the slower moving separation buffer zone and to slow down the faster moving background buffer zone to an average flow velocity, $\bar{u}_{eo}$. This is connected with a parabolic flow profile distortion in both buffer zones. In the separation buffer zone, the distortion is directed towards the cathode and in the background buffer zone towards the anode (for details see Ref. [16]).

For the average flow velocity, $\bar{u}_{eo}$, follows:

$$\bar{u}_{eo} = u_{eo,SB} + u_{hd,SB} = u_{eo,BB} + u_{hd,BB} \quad (1)$$

where $u_{hd,SB}$ and $u_{hd,BB}$ are the laminar flow components in the respective buffer zones caused by $p_i$. Their magnitude can be calculated by the Hagen–Poiseuille equation [32]:

$$u_{hd,SB} = +\frac{r^2 p_i}{8\eta L_{SB}} \quad (2)$$

and

$$u_{hd,BB} = -\frac{r^2 p_i}{8\eta L_{BB}} \quad (3)$$

where $r$ is the inner capillary radius, $\eta$ is the viscosity and $L_{SB}$ and $L_{BB}$ are the lengths of the buffer zones. If the direction of the electroosmotic flow is designated to be positive, $u_{hd,SB}$ (directed towards the cathode) has a positive sign and $u_{hd,BB}$ (directed towards the anode) has a negative sign. The intersegmental pressure, $p_i$, can be estimated by combining Eqs. (1)–(3):

$$p_i = \frac{8\eta L_{SB} L_{BB}}{r^2 L_{total}} \cdot (u_{eo,BB} - u_{eo,SB}) \quad (4)$$

where the total capillary length, $L_{total}$, is the sum of $L_{SB}$ and $L_{BB}$. The amount of the laminar flow component in each buffer zone can be calculated using Eqs. (2) and (3), respectively.

As shown in Eq. (4), $p_i$ increases with increasing difference of the electroosmotic flow velocities and is maximum for a given total capillary length if $L_{SB} = L_{BB}$. For a given ratio of $L_{SB}$ and $L_{BB}$ $p_i$ increases with increasing capillary length $L_{total}$. As the length of the separation buffer zone is not constant during the run, $L_{SB}$ and $L_{BB}$ change with proceeding migration time, $t_M$. Consequently, $p_i$ and hence the laminar flow components will also change

during the run. Knowing the flow velocity of the boundary between the separation buffer zone and the background buffer zone, $u_{bou}$, the zone lengths, $L_{SB,t_M}$, at the time of detection of an analyte, $t_M$, can be estimated using Eq. (5):

$$L_{SB,t_M} = L_{SB,t_M=0} + u_{bou} t_M \quad (5)$$

$p_i$ will become zero if $L_{SB,t_M} = L_{total}$. Therefore, $u_{hd,SB}$ and $u_{hd,BB}$ will be zero, too.

For the interpretation of plate numbers it must be taken into consideration that on their way from the injection end to the detection window the analytes migrate under the influence of different flow profiles. As discussed earlier [16], the flow profile in the separation buffer zone has a major influence on the efficiency because a parabolically distorted flow profile gives rise to an increased contribution of mass transfer to plate height [33].

## 3. Experimental

### 3.1. Buffer systems and chemicals

Buffer solutions were prepared from analytical-grade chemicals (Merck, Darmstadt, Germany). Borate buffer was exclusively used in this work. A stock solution was prepared having a concentration of 0.1 *M* with boric acid and adjusted to pH 9.4 with 1 *M* sodium hydroxide solution. For all experiments, the separation buffer was prepared diluting the borate buffer to 15 m*M* with water and methanol (90:10, v/v), then SDS (Roth, Karlsruhe, Germany) was added to give a concentration of 15 m*M*. For the background buffer the borate buffer was diluted to a concentration of 10 m*M* with water and methanol (90:10, v/v).

For partial filling measurements with equalized electroosmotic flow velocities the separation buffer was used as above. The needed background buffer having the same electroosmotic flow (EOF) as the separation buffer was estimated from a series of differently concentrated borate buffers. It was prepared as described above at a concentration of 17.77 m*M* borate and 10% (v/v) methanol.

Acetone (Promochem, Wesel, Germany) was used as EOF marker. The homologous ω-phenylalcohols (benzyl alcohol to ω-phenylhexanol, abbreviated as 1–6) used as test compounds were obtained from Fluka and Aldrich (Deisenhofen, Germany) and injected at concentrations of about 300 μg/ml in the separation buffer. Decanophenone (Aldrich) was used as micelle marker (MC) at a concentration of about 160 μg/ml. It was also employed as a marker for the separation buffer zone at a concentration of about 20 μg/ml.

All solutions were prepared using water purified by an Elgastat-UHQPS system (USF Elga, Ransbach-Baumbach, Germany), and filtered with 0.2-μm syringe filters (Schleicher & Schuell, Dassel, Germany).

### 3.2. CE system

All experiments were performed with a PRINCE system (injection device with high-voltage power supply; Prince Technologies, Emmen, The Netherlands). Accurate counter pressures were achieved using an ER 3000 electropneumatic pressure controller (Dräger Tescom, Lübeck, Germany).

For detection, a Jasco 875-CE UV detector (Tokyo, Japan) and for data evaluation the personal computer-based integration software Gynkosoft version 4.22 (Dionex Softron, Germering, Germany) were used.

Plain fused-silica capillaries, 100 cm×50 μm I.D. and 150 cm×50 μm I.D., 365 μm O.D. (MicroQuartz, Munich, Germany) were applied. The effective capillary length was 77 cm in both cases. Detection was carried out on-capillary at 254 nm for acetone and at 205 nm for the ω-phenylalcohols.

### 3.3. Procedures

Determination of the necessary injection time of the separation buffer for the 150 cm and 100 cm long capillaries was carried out as follows (values for the 100 cm capillary in parentheses): the capillary was first flushed with 0.2 *M* NaOH for 6 min (4 min) at 1000 mbar followed by rinsing with the background buffer for 6 min (4 min) at 1000 mbar. Subsequently, the marked separation buffer was injected at 450 mbar and at the same time the baseline was monitored at 205 nm until the breakthrough of the separation buffer at the detection window occurred.

The breakthrough could be seen by an increasing baseline. Based on this breakthrough time the injection time necessary to fill a capillary length of 60 cm was calculated to be 5.50 min for the 150 cm long capillary and 3.54 min for the 100 cm long capillary (3.62 min for the buffer combination with equalized EOFs) which corresponds to a filling degree of 40% and 60% related to total capillary length. A scheme representing the buffer constellation, the initial filling degree, and the initial flow profile distortion in each buffer zone is given in Fig. 1.

Before each run in the partial filling mode, the capillary was rinsed with 0.2 *M* NaOH for 6 min (4 min) and background buffer for 6 min (4 min) at 1000 mbar followed by the injection of the separation buffer at 450 mbar for the times given above. During the run, the inlet-vial contained the separation buffer and the outlet-vial contained the background buffer in order to avoid further zone boundaries. The buffer in the outlet-vial was replaced before each run. In one of three equal runs the separation buffer was marked with a small amount of the micelle marker decanophenone to visualize the boundary between the separation buffer zone and the background buffer zone in the electropherograms.

Plate numbers of the ω-phenylalcohols were measured on both capillaries without (0 mbar) and with the application of counter pressures of 5, 10, 20 and 30 mbar, respectively, at a field strength of 200 V/cm (30 kV for the 150 cm capillary and 20 kV for the 100 cm capillary). Injection of the sample (10 mbar/0.1 min) was carried out hydrodynamically.

The data for a particular capillary system at different counter pressures were evaluated by graphs plotting the theoretical plate number $N$ vs. the effective velocity $u_{\mathrm{eff}}$ of the analytes. For better comparison the same scale was chosen for all graphs. $N$ was directly taken from the Gynkosoft program which uses Eq. (6) for its calculation ($t_{\mathrm{M}}$ is the measured migration time of the respective analyte and $w_{0.5}$ is the measured peak width at half height):

$$N = 5.54 \cdot \left( \frac{t_{\mathrm{M}}}{w_{0.5}} \right)^2 \tag{6}$$

The discussed values are the mean of three

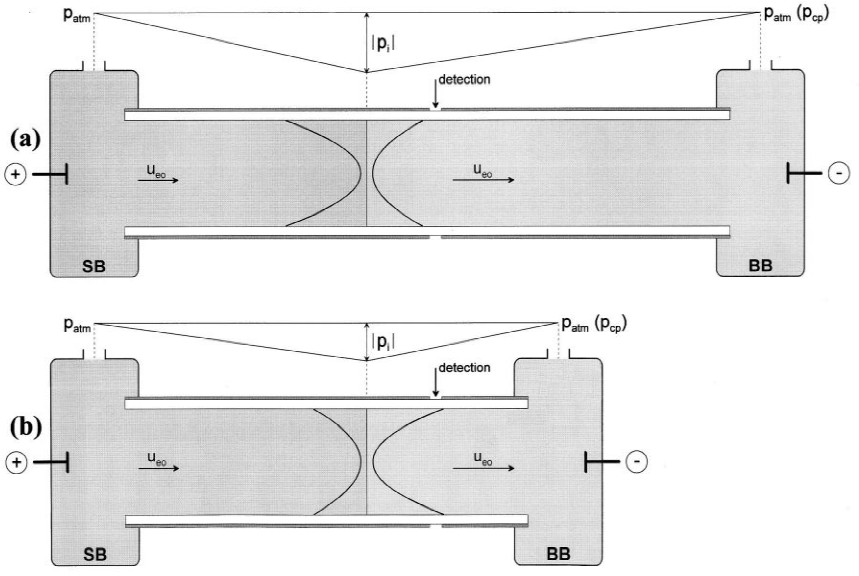


Fig. 1. Scheme of the experimental setup: (a) 150 cm capillary, 40% initial filling degree and (b) 100 cm capillary, 60% initial filling degree using a buffer constellation with $u_{\mathrm{eo,SB}} < u_{\mathrm{eo,BB}}$. The pressure constellations are depicted upon the capillaries ($p_{\mathrm{atm}}$ = ambient pressure, $p_{\mathrm{i}}$ = intersegmental pressure, $p_{\mathrm{cp}}$ = optional counter pressure applied at the cathodic side). The initial flow profiles induced by $p_{\mathrm{i}}$ are shown in the respective buffer zones (——).

Table 1
Electroosmotic flow velocities of the buffers and velocity of the zone boundary at different counter pressures used for the calculation of $p_i$, $u_{hd,SB}$ and $u_{hd,BB}$

| | $L_{total}$ (cm) | $u_{eo,SB}$ (mm/s) | $u_{eo,BB}$ (mm/s) | $u_{bou,0\ mbar}$ (mm/s) | $u_{bou,10\ mbar}$ (mm/s) | $u_{bou,30\ mbar}$ (mm/s) |
|---|---|---|---|---|---|---|
| 100 cm capillary | 100 | 0.81 | 0.93 | 0.38 | 0.25 | 0.06 |
| 150 cm capillary | 150 | 0.83 | 0.96 | 0.47 | 0.40 | 0.31 |

Further parameters: $L_{SB,t_M=0}=60$ cm; $\eta=9.89\cdot10^{-4}$ Pa s; $r=25\cdot10^{-6}$ m.

measurements. Relative mean standard errors for a series of values measured at a given counter pressure were calculated according to Ref. [34] based on the standard error of the triple determination for each component [34]. The relative mean standard errors of the plate numbers measured on the 100 cm capillary are: 5.4% (0 mbar), 7.5% (5 mbar), 4.0% (10 mbar), 6.1% (20 mbar) and 7.1% (30 mbar). Values for the 150 cm capillary are: 5.1% (0 mbar), 7.3% (5 mbar), 6.0% (10 mbar), 4.2% (20 mbar) and 6.7% (30 mbar).

$u_{eff}$ was calculated using Eq. (7) ($L_{eff}$ is the capillary length to the detection window):

$$u_{eff}=\frac{L_{eff}}{t_M}\quad (mm/s) \tag{7}$$

A second type of graphs was used to show the course of the intersegmental pressure, $p_i$, and the laminar flow profile components, $u_{hd,SB}$ and $u_{hd,BB}$, during the run. The curves were calculated using the equations developed in Section 2 (values used for calculation see Table 1). Below the curves, plate numbers of the alcohols 1, 4 and 6 are depicted as bars at the time of detection. Thereby, it becomes obvious which flow profiles govern its separation process. $u_{eo,SB}$ and $u_{eo,BB}$ were measured with acetone as EOF marker in the capillaries completely filled with the respective buffer. $u_{bou}$ was calculated using the breakthrough times of the separation buffer zone in the electropherograms for different counter pressures.

## 4. Results and discussion

Plate numbers $N$ of the homologous ω-phenylalcohols 1–6 were measured on two different capillaries, 150 cm and 100 cm in length, applying the PF-MEKC mode under identical conditions [SB: 15 m*M* SDS, 15 m*M* borate, 10% (v/v) MeOH; BB: 10 m*M* borate, 10% (v/v) MeOH; initial separation buffer zone length: 60 cm; field: 200 V/cm] without and with the application of counter pressures.

The measured plate numbers are plotted vs. the effective mobilities $u_{eff}$ of the ω-phenylalcohols in Fig. 2a (100 cm capillary) and Fig. 2b (150 cm capillary). Plate numbers on the 100 cm capillary without counter pressure come up to 160 000–210 000 for the homologous alcohols. By the application of weak counter pressures of 5 and 10 mbar, plate numbers are slightly increased by about 5000–30 000 plates. A further increase of counter pressure leads to a sharp drop of plate numbers. At a counter pressure of 30 mbar plate numbers are in a range of 110 000–130 000 for the alcohols 1–4 and 50 000 and 75 000 for the alcohols 5 and 6, respectively. As shown in Fig. 2b plate numbers on the 150 cm capillary (about 130 000 for the alcohols 1–3 and 75 000–110 000 for the alcohols 4–6) are generally lower than those on the 100 cm capillary (Fig. 2a). The application of counter pressure does not lead to great changes. Counter pressures of 20 and 30 mbar results in a slight increase of plate numbers of about 5000 up to 40 000 plates.

The lower plate numbers obtained on the 150 cm capillary are also obvious in the electropherograms shown in Fig. 3a and b where all test components are detected in the separation buffer zone on both capillary systems. In case of the 100 cm capillary a counter pressure of 30 mbar (Fig. 3c) delays the movement of the separation buffer zone such that the alcohols 1–5 are detected in the background buffer zone and alcohol 6 at the boundary. Peak widths and plate numbers are similar for both capillary systems at 30 mbar counter pressure.

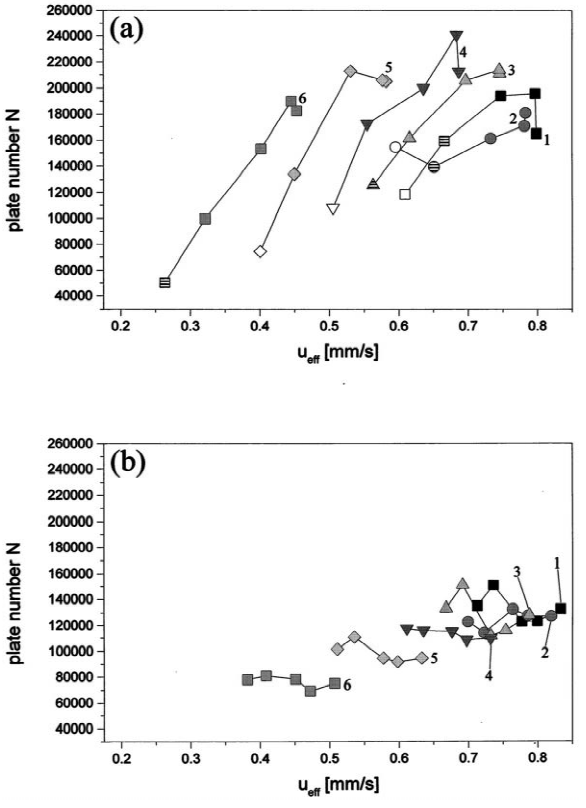


Fig. 2. Plate numbers vs. effective velocities for (a) the 100 cm capillary and (b) the 150 cm capillary. Conditions: buffers, field, detection and filling degree: see Experimental; compounds (from right to left): ■ benzyl alcohol (1), ● ω-phenylethanol (2), ▲ ω-phenylpropanol (3), ▼ ω-phenylbutanol (4), ♦ ω-phenylpentanol (5), ■ ω-phenylhexanol (6); symbol fillings: full symbols: detection in the separation buffer zone, striped symbols: detection together with the boundary between separation and background buffer zone, open symbols: detection in the background buffer zone; counter pressure: increasing counter pressure (0, 5, 10, 20, 30 mbar) is represented by decreasing $u_{\mathrm{eff}}$ in each data set.

### *4.1. 100 cm capillary, 60% initial filling degree of the separation buffer*

In Fig. 4, the course of the intersegmental pressure, $p_{\mathrm{i}}$ and the trend of the laminar flow components, $u_{\mathrm{hd,SB}}$ and $u_{\mathrm{hd,BB}}$, which is equivalent to the parabolic flow profile distortion in the separation buffer zone and the background buffer zone, respectively, are plotted against the run time. Under it, the plate numbers for the ω-phenylalcohols 1, 4 and 6 are shown as bars over their migration times to illustrate under which flow conditions the analytes migrated and in which buffer zone they are detected. The corresponding electropherograms are shown in Fig. 3.

At 0 mbar counter pressure, all phenylalcohols are detected in the separation buffer (Fig. 4a) which means $u_{\mathrm{hd,BB}}$ is ruled out to contribute to peak broadening. Plate numbers are solely influenced by the flow profile of the separation buffer zone. At the beginning of the run, the intersegmental pressure was calculated to have a value of 3.82 mbar which induces a laminar flow component of $u_{\mathrm{hd,SB}} = 0.05$ mm/s in the separation buffer and an appropriate parabolic distortion of the flow profile. In the later course of the run this distortion decreases with decreasing $p_{\mathrm{i}}$ as the separation buffer zone becomes longer. After about 17.8 min the capillary is completely filled with separation buffer and $p_{\mathrm{i}}$ and the flow profile distortion becomes zero. As a consequence the migration of phenylalcohol 1 (165 000 plates) is governed all the time until detected by a distorted profile. Phenylalcohol 4 undergoes no distortion (plug like profile) for a very short period before detection. Alcohol 6 migrates nearly half of its run time under plug like flow conditions. Proportionate, plate numbers are higher for the alcohols 4 and 6 (210 000 and 180 000). Using counter pressures of 5 and 10 mbar these alcohols are still detected in the separation buffer zone. A counter pressure of 5 mbar just compensates for the flow profile distortion of the separation buffer zone and plate numbers increase as shown in Fig. 2a. At a counter pressure of 10 mbar the capillary is completely filled with the separation buffer after 26.8 min (Fig. 4b). Because the migration times of the phenylalcohols 1 and 4 are smaller, they migrate in the separation buffer zone under the influence of the superposition of two parabolic profiles: the parabolic profile induced by the intersegmental pressure in cathodic direction is compensated or overcompensated by the anodically directed parabolic flow profile caused by counter pressure. Therefore, plate numbers obtained are similar to those measured without the application of counter pressure. Phenylalcohol 6 migrates a shorter period of time in the non-distorted separation buffer zone compared to the case without counter pressure which explains the lower plate number. Application of higher counter

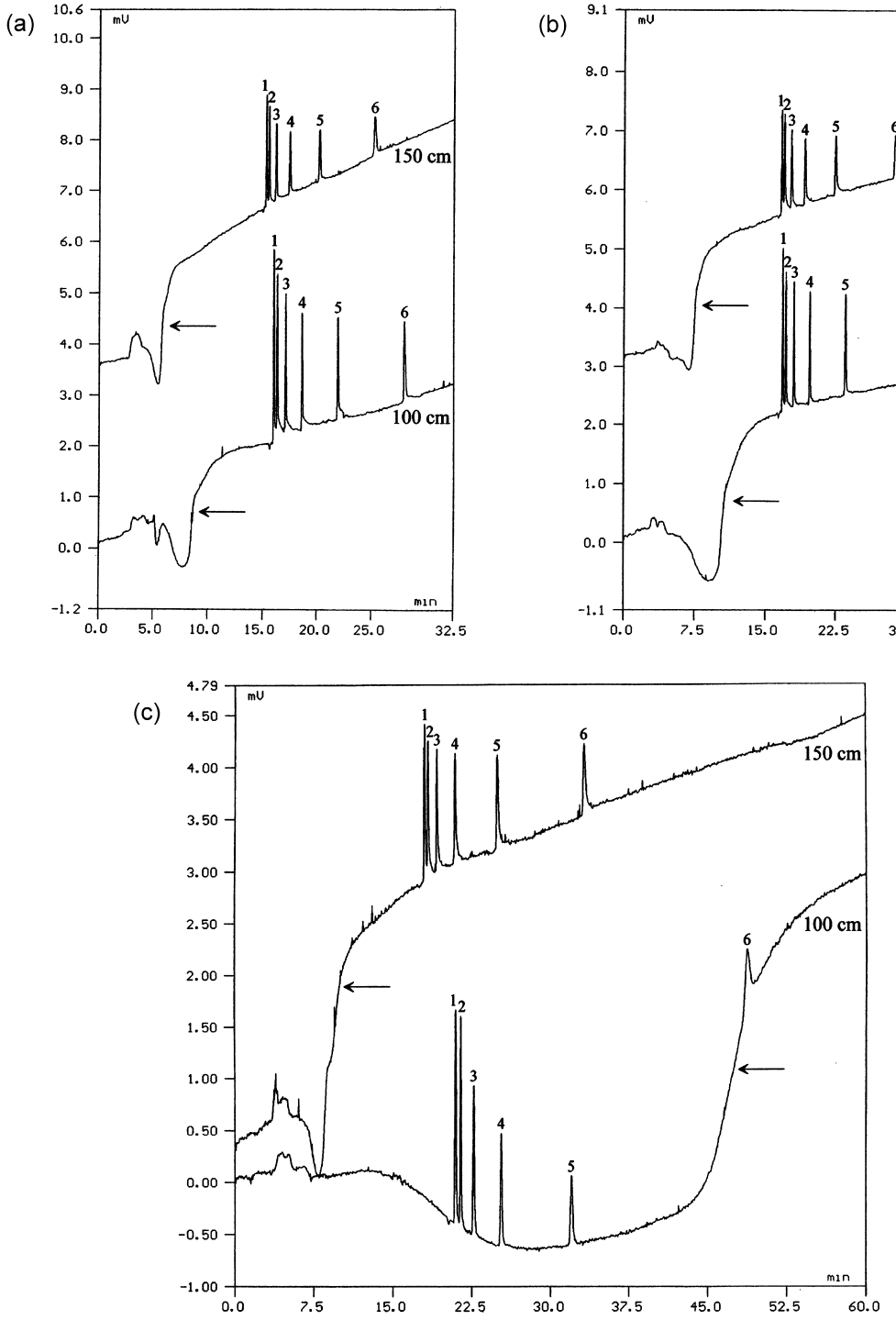


Fig. 3. Electropherograms obtained on the 100 cm and the 150 cm capillary applying a counter pressure of (a) 0 mbar, (b) 10 mbar and (c) 30 mbar. Conditions: buffers, field, detection and filling degree: see Experimental; compounds: homologous ω-phenylalcohols from (1) benzyl alcohol to (6) ω-phenylhexanol. The increase of the baseline (marked with an arrow) indicates the breakthrough of the separation buffer zone at the detection window.

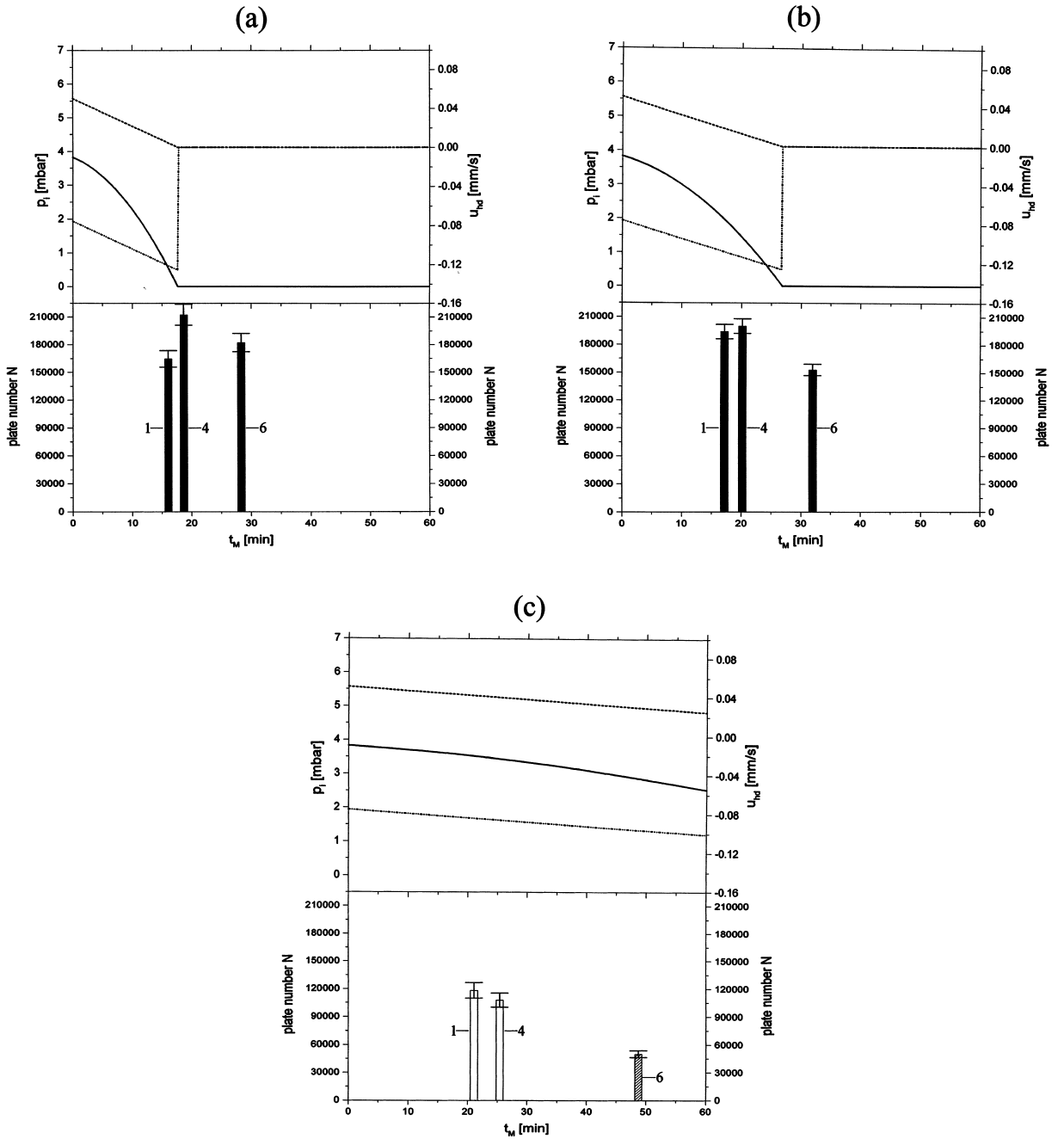


Fig. 4. Course of the intersegmental pressure and the laminar flow component in the buffer zones (upper plots) and plate numbers for (bars from left to right) benzyl alcohol (1), ω-phenylbutanol (4), ω-phenylhexanol (6) on the 100 cm capillary in dependence on the run time at a counter pressure of (a) 0 mbar, (b) 10 mbar and (c) 30 mbar. Values for calculation: see Table 1; line explanations: (——) intersegmental pressure $p_i$, (- - -) laminar flow component in the separation buffer zone, $u_{hd,SB}$, caused by $p_i$, (•• - •• - ••) laminar flow component in the background buffer zone, $u_{hd,BB}$, caused by $p_i$; filling of the bars: full bars: detection in the separation buffer zone, striped bars: detection together with the boundary between separation and background buffer zone, open bars: detection in the background buffer zone.

pressures further delays the movement of the zone boundary. At a counter pressure of 30 mbar the capillary is never completely filled with the separation buffer within the migration time of the six phenylalcohols (Fig. 4c). In this case the alcohols 1 and 4 are detected in the background buffer zone while alcohol 6 is detected at the boundary of the two buffer zones (see also the electropherogram in Fig. 3c). Compared to a counter pressure of 10 mbar, plate numbers are considerably reduced to about 50 000–120 000 plates. This decrease can be explained by two effects: The cathodic laminar flow component of the separation buffer zone is overcompensated by the laminar counter flow component which effects a reversed parabolic flow profile distortion directed to the anode affecting all alcohols. In addition, the anodically directed parabolic flow profile distortion of the background buffer zone increases during the run due to the decreasing zone length and is further increased by the counter pressure induced flow component. As the alcohols 1 and 4 are detected in the background buffer zone, the latter effect may be involved in low plate numbers for these components.

### *4.2. 150 cm capillary, 40% initial filling degree of the separation buffer*

By analogy with Fig. 4 the courses of $p_i$, $u_{hd,SB}$, and $u_{hd,BB}$ are plotted versus the run time for the 150 cm capillary in Fig. 5 (for the corresponding electropherograms see Fig. 3). All phenylalcohols are detected in the separation buffer zone at all counter pressures applied. Therefore peak broadening can be attributed solely to the flow profile distortion in the separation buffer zone. As it became obvious already by Fig. 2 plate numbers are generally lower but less dependent on counter pressure in case of the 150 cm capillary. This can be explained by several effects: The initial intersegmental pressure (6.09 mbar) is about 60% higher when using the 150 cm capillary which causes a laminar flow component of $u_{hd,SB} = 0.08$ mm/s in the separation buffer zone. Consequently, the analytes are exposed to a higher flow profile distortion compared to the 100 cm capillary which explains the lower plate numbers of 75 000–130 000. Identical counter pressures $p_{cp}$ induce lower laminar flow components in the 150 cm capillary (see Eq. (3), using $p_{cp}$ instead of $p_i$ and $L_{total}$ instead of $L_{BB}$). Therefore, the compensation of the cathodic flow profile deformation is delayed and consequently the increase of plate numbers must be shifted towards higher counter pressures. This explanation is supported by the slight increase of plate numbers when applying counter pressures of 20 to 30 mbar but it may also reflect the uncertainty of the measurement of plate numbers.

That the influence of counter pressure is much less pronounced in case of a longer capillary becomes also evident looking on the migration time windows, $t_{MC}/t_0$, given in Table 2. Increasing the counter pressure from 0 to 30 mbar, $t_{MC}/t_0$ is increased by at least 125% in case of the 100 cm capillary but only 63% in case of the 150 cm capillary. This can also be seen in the electropherograms recorded at a counter pressure of 30 mbar (Fig. 3c). The breakthrough of the separation buffer zone occurs much later in case of the 100 cm capillary.

The observed effects can be explained satisfactorily by the discussed flow profile models although some further phenomena are not taken into account, e.g., the slightly different electric field strengths in the buffer zones: The separation buffer has a lower specific resistance than the background buffer because of its higher concentration. Therefore, the field strength will not be uniform over the whole capillary. It will be lower in the separation buffer and higher in the background buffer. This may influence the electroosmotic flow velocities of the buffer zones to a certain extent. Consequently, changing buffer zone lengths will alter the electric field strengths during the run. By this effect the value of $u_{hd,SB}$ will be higher at the beginning of a run but the decrease of $u_{hd,SB}$ will be somewhat faster.

Some consequences can be derived: long background buffer zones should be avoided if the electroosmotic flow velocities of the buffer zones are not exactly matched. Consequently, the application of counter pressure as a tool to slow down the movement of the separation buffer zone in order to increase the migration time window and to compensate for parabolic flow profile distortions requires higher counter pressures.

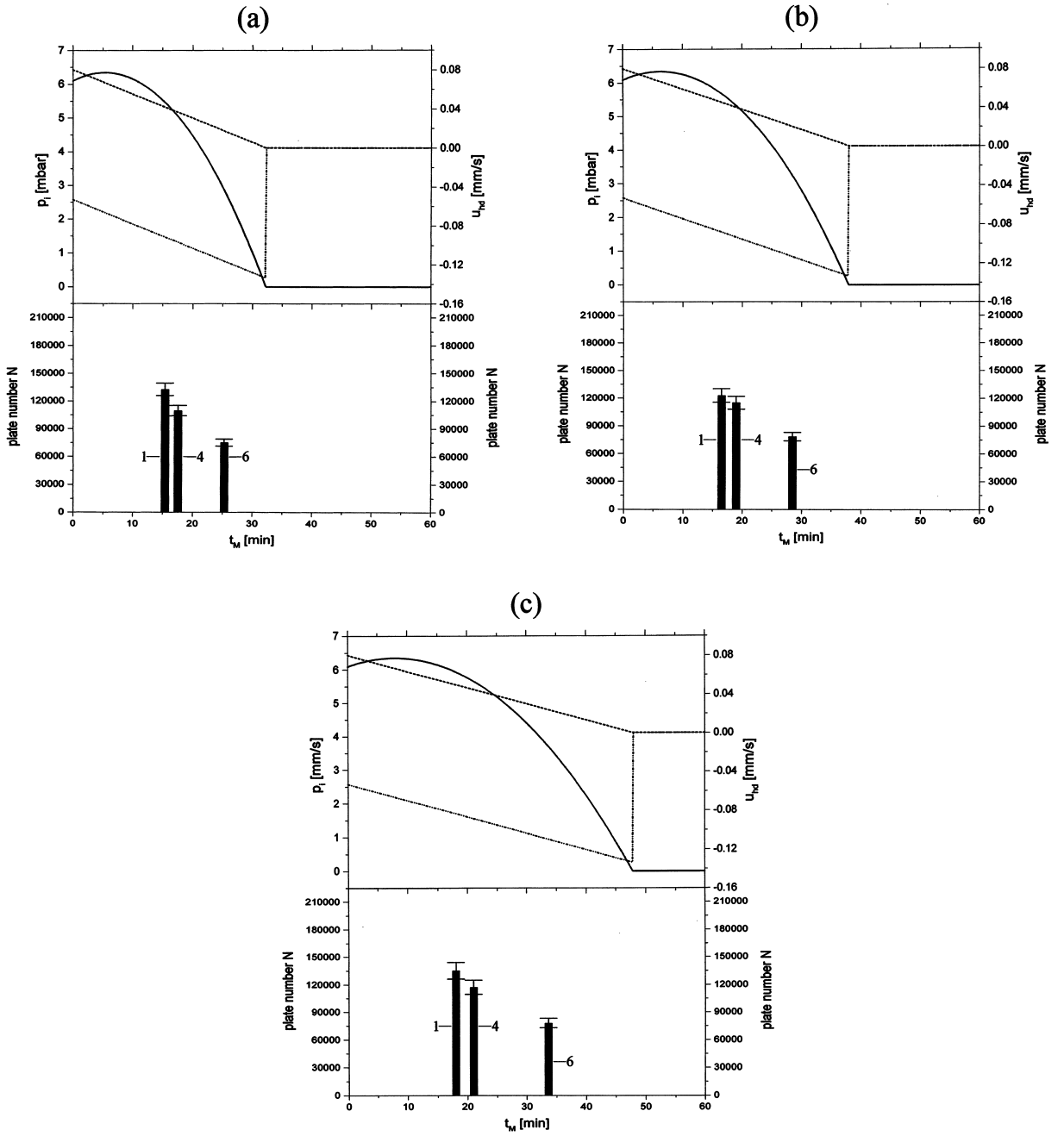


Fig. 5. Course of the intersegmental pressure and the laminar flow component in the buffer zones (upper plots) and plate numbers for (bars from left to right) benzyl alcohol (1), ω-phenylbutanol (4), ω-phenylhexanol (6) on the 150 cm capillary in dependence on the run time at a counter pressure of (a) 0 mbar, (b) 10 mbar and (c) 30 mbar. Values for calculation: see Table 1; line explanations and filling of bars: see Fig. 4.

Table 2
Table of the migration time windows expressed by $t_{MC}/t_0$ for both capillary systems applying different counter pressures

| Counter pressure (mbar) | 100 cm capillary $t_{MC}/t_0$ | 150 cm capillary $t_{MC}/t_0$ |
|---|---|---|
| 0 | 3.27 | 2.94 |
| 5 | 3.69 | 3.25 |
| 10 | 4.22 | 3.48 |
| 20 | >6.41* | 4.07 |
| 30 | >7.33* | 4.78 |

*The micelle marker was not detected until the end of the run.

### *4.3. 100 cm capillary with equalized electroosmotic flows of the buffers, 60% initial filling degree of the separation buffer*

As reported in a previous paper [16] a partial filling system supplies best efficiencies if the electroosmotic flow velocities of the two buffers are equalized. This case was realized on the 100 cm capillary using a buffer combination of a separation buffer as above and a background buffer containing 17.77 m*M* borate and 10% (v/v) MeOH. Because of the absence of parabolic flow profile distortions plate numbers are expected to be higher than on the same capillary filled with the mismatched buffers [10 m*M* borate and 10% (v/v) MeOH as background buffer]. The obtained plate numbers are shown in Fig. 6. Without counter pressure plate numbers come to 230 000–350 000 which is indeed significantly higher. With increasing counter pressure plate numbers are reduced step by step due to the parabolic distortion of the initial plug profile. Using 30 mbar counter pressure plate numbers are in a range of 110 000–130 000 for the alcohols 1–3 and 50 000–90 000 for the alcohols 4–6 which is comparable to the values obtained in case of mismatched electroosmotic flows.

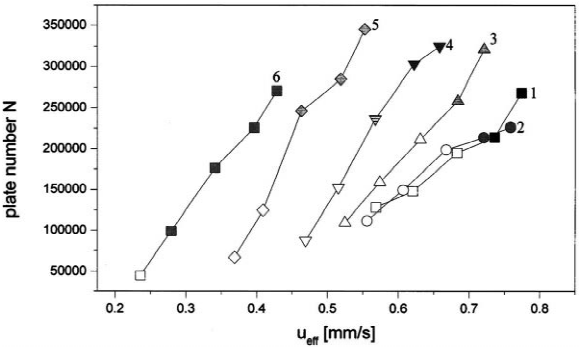


Fig. 6. Plate numbers vs. effective velocities for the 100 cm capillary in case of equalized electroosmotic flows. Conditions: buffers, field, detection and filling degree: see Experimental; compounds, symbol fillings and counter pressure: see Fig. 2.

## 5. Conclusions

It was shown that when using counter pressure moderated PF-MEKC, an intersegmental pressure caused by mismatched electroosmotic flows of the buffer plugs does not only depend on the magnitude of these differences but also on the relative buffer zone lengths and the total length of the capillary. As the buffer zone lengths change during the run, the intersegmental pressure and hence the laminar flow components which are responsible for flow profile distortions also change. Counter pressure applied to delay the movement of the zone boundary towards the detection window induces laminar flow components as well which superpose the intersegmental pressure induced laminar flow components. Consequently, the analytes migrate under varying parabolically distorted flow profiles during their way from the injection end to the detection window which strongly influences plate numbers. In case of a short background buffer zone the parabolic flow profile distortion in the separation buffer is smaller and counter pressure has a significant influence on efficiency. Plate numbers can be increased by the application of weak counter pressures because of a reduction of the parabolic flow profile distortion. Higher counter pressures inverse the flow profile with the consequence of decreasing plate numbers. Using the longer capillary but the same initial separation zone length the intersegmental pressure is higher and hence a larger parabolic flow profile distortion results in the separation buffer zone. The outcome are lower plate numbers. When applying weak counter pressures, plate numbers stay nearly constant as the effect of counter pressure decreases with increasing capillary length or with other words compensation of the parabolic flow profile distortion in the separation buffer zone requires higher counter pressures. These studies showed again that best plate

numbers are obtained if the electroosmotic flows of the buffer zones are equalized.

## Acknowledgements

Support for this work by the German Science Foundation is gratefully acknowledged (DFG-We 1829).

## References

[1] S. Terabe, K. Otsuka, K. Ichikawa, A. Tsuchiya, T. Ando, Anal. Chem. 56 (1984) 111.
[2] S. Terabe, H. Ozaki, K. Otsuka, T. Ando, J. Chromatogr. 332 (1985) 211.
[3] J.H.T. Luong, Y. Guo, J. Chromatogr. A 811 (1998) 225.
[4] N. Tanaka, T. Tanigawa, K. Hosoya, K. Kimata, T. Araki, S. Terabe, Chem. Lett. 6 (1992) 959.
[5] A.L. Gray, J.T. Hsu, J. Chromatogr. A 824 (1998) 119.
[6] C.P. Palmer, H.M. McNair, J. Microcol. Sep. 4 (1992) 509.
[7] C.P. Palmer, S. Terabe, J. Microcol. Sep. 8 (1996) 115.
[8] F. Haddadian, S.A. Shamsi, I.M. Warner, Electrophoresis 20 (1999) 3011.
[9] H. Ozaki, S. Terabe, A. Ichihara, J. Chromatogr. A 680 (1994) 117.
[10] N. Tanaka, K. Nakagawa, K. Hosoya, C.P. Palmer, S. Kunugi, J. Chromatogr. A 802 (1998) 23.
[11] B. Potoček, B. Maichel, B. Gaš, M. Chiari, E. Kenndler, J. Chromatogr. A 798 (1998) 269.
[12] J.P. Kutter, T. Welsch, J. High Resolut. Chromatogr. 18 (1995) 741.
[13] T. Welsch, S. Kolb, J.P. Kutter, J. Microcol. Sep. 9 (1997) 15.
[14] S. Kolb, J.P. Kutter, T. Welsch, J. Chromatogr. A 792 (1997) 151.
[15] S. Kolb, T. Welsch, J.P. Kutter, J. High Resolut. Chromatogr. 21 (1998) 435.
[16] D. Michalke, S. Kolb, T. Welsch, J. Chromatogr. A 916 (2001) 113.
[17] D. Shohat, E. Grushka, Anal. Chem. 66 (1994) 747.
[18] K. Bächmann, A. Bazzanella, I. Haag, K.-Y. Han, R. Arnecke, V. Böhmer, W. Vogt, Anal. Chem. 67 (1995) 1722.
[19] L. Valtcheva, J. Mohammad, G. Pettersson, S. Hjertén, J. Chromatogr. 638 (1993) 263.
[20] Y. Tanaka, S. Terabe, J. Chromatogr. A 694 (1995) 277.
[21] W.M. Nelson, Q. Tang, A.K. Harrata, C.S. Lee, J. Chromatogr. A 749 (1996) 219.
[22] Y. Tanaka, Y. Kishimoto, S. Terabe, J. Chromatogr. A 802 (1998) 83.
[23] R.-L. Chien, J.C. Helmer, Anal. Chem. 63 (1991) 1354.
[24] U. Bütehorn, U. Pyell, Chromatographia 43 (1996) 237.
[25] W.M. Nelson, C.S. Lee, Anal. Chem. 68 (1996) 3265.
[26] A. Amini, U. Paulsen-Sörman, D. Westerlund, Chromatographia 50 (1999) 497.
[27] J.K. Towns, F.E. Regnier, Anal. Chem. 64 (1992) 2473.
[28] C.A. Keely, T.A.A.M. van de Gor, D. McManigill, Anal. Chem. 66 (1994) 4236.
[29] B. Potoček, B. Gaš, E. Kenndler, M. Štědrý, J. Chromatogr. A 709 (1995) 51.
[30] A.E. Herr, J.I. Molho, J.G. Santiago, M.G. Mungal, T.W. Kenny, M.G. Garguilo, Anal. Chem. 72 (2000) 1053.
[31] A.S. Rathore, Cs. Horváth, Anal. Chem. 70 (1998) 3069.
[32] F.W. Sears, M.W. Zemansky, H.D. Young, University Physics, 5th ed., Addison-Wesley, Reading, MA, 1976, p. 243.
[33] J.H. Knox, Chromatographia 26 (1988) 329.
[34] M. Otto, in: Chemometrics: Statistics and Computer Application in Analytical Chemistry, Wiley–VCH, Weinheim, 1999, p. 21;
M. Otto, in: Chemometrics: Statistics and Computer Application in Analytical Chemistry, Wiley–VCH, Weinheim, 1999, p. 286.